Chapter 6

β-Xylosidase and transxylosidase activities of human glucocerebrosidase

β-Xylosidase and transxylosidase activities of human glucocerebrosidase

D.E.C. Boer, M. Mirzaian, M.J. Ferraz, K.C. Zwiers, M. Hazeu, M.V. Baks, R. Ottenhoff, A.R.A. Marques, R. Meijer, J.C.P. Roos, T. Cox, R.G. Boot, N.j. Pannu, H.S. Overkleeft, M.E. Artola, J.M.F.G. Aerts.

Abstract

Glucocerebrosidase (GCase) is a lysosomal retaining β-glucosidase that hydrolyzes β-glucosidic substrates and transglucosylates cholesterol to cholesterol-β-glucoside (GlcChol). Here we demonstrate that recombinant human GCase also cleaves 4-methylumbelliferyl-β-D-xylose (4-MU-β-Xyl) and is able to transxylosylate cholesterol. Formed xylosyl-cholesterol (XylChol) acts as subsequent acceptor to render di-xylosyl-cholesterol. Examination of mutant forms of GCase from Gaucher disease patients revealed no marked abnormalities in relative β-glucosidase, β-xylosidase, transglucosidase and transxylosidase activities. The presence of low levels of XylChol in mouse and human tissue was detected and its origin studied. Intact cultured cells were found to form XylChol, in GCase dependent manner, when exposed to 4-MU-β-Xyl or a plant-derived cyanidine-β-xyloside. Unlike GCase, the cytosol-facing β-glucosidase GBA2 shows no β-xylosidase or transxylosidase activity. Likewise glucosylceramide synthase (GCS) is unable to synthesize XylChol. Next, we detected xylosylated ceramide (XylCer) in tissues. XylCer was found to also act as donor in XylChol formation by GCase. Unexpectedly, GCS was observed to be able to generate XylCer. Thus, food derived β-D-xyloside and XylCer are potential donors for GCase driven formation of XylChol in cells and tissues formed via transxylosylation by GCase. In conclusion, our findings point to further catalytic versatility of GCase and warrant examination of occurrence and function of xylosylated lipids.

Introduction

The aldopentose xylose resembles the six-membered cyclic pyranose glucose except for lacking the pendant CH2OH group. As main building block of xylan, xylose is a major plant sugar [1]. In animals xylose is added

by uridine diphosphate D-xylose (UDP-Xyl) dependent xylosyltransferases as the first saccharide to sidechain hydroxyls of serine or threonine residues during O-glycosylation of proteoglycans. This step is essential in synthesis of glycosaminoglycans like heparan sulfate, keratan sulfate and chondroitin sulfate [2]. The human body is unable to synthesize xylose de novo. UDP-Xyl is however formed from UDP-glucuronate by UDP-glucuronic acid decarboxylase 1 encoded by the UXS1 gene [3]. Since the first investigations by Fisher & Kent and Patel & Tappel in the late sixties, degradation of β-xylosides in animals is thought to rely on β-glucosidases [4, 5]. This does not come as a surprise in view of the structural similarity of xylose with glucose. We earlier demonstrated that indeed the lysosomal acid β-glucosidase GCase, also known as glucocerebrosidase, hydrolyzes 4-methylumbelliferyl-β-xyloside (4-MU-β-Xyl), in contrast to the non-lysosomal β-glucosidase GBA2 [6]. Inherited defects in GCase cause Gaucher disease (GD), a progressive disorder characterized by the accumulation of macrophages loaded with glucosylceramide (GlcCer) in tissues [7, 8]. No accumulation of β-D-xylose-containing glycopeptides in GD patients has been reported, but this possibility has not been actively studied. More recently another catalytic capacity of GCase has been recognized: the transfer of glucose from β-glucoside substrates to cholesterol, thus generating glucosyl-β-D-cholesterol (GlcChol) [9-11]. Generation of GlcChol by GCase is not merely a test tube phenomenon, but also takes place *in vivo* [10]. In Niemann Pick type C disease (NPC), intralysosomal cholesterol is markedly increased due to genetic defects in any of the two proteins NPC1 or NPC2 mediating the egress of the sterol from lysosomes [12]. During this pathological condition, GCase actively generates GlcChol [10]. Formation of GlcChol can also be experimentally induced by incubating cells with U18666A, an inhibitor of efflux of cholesterol from lysosomes. The transglucosylation reaction in cells is prohibited by concomitant inhibition of GCase [10]. The β-glucosidase GBA2, tightly associated to the cytoplasmic leaflet of membranes, also exerts transglucosidase activity *in vitro* and *in vivo* [10, 13-15].

The earlier findings on glycon substrate specificity of GCase and the recently noted transglucosidase activity of the enzyme prompted us to examine whether GCase is also able to generate xylosyl-β-D-cholesterol (XylChol). We here report on the *in vitro* xylosylation of cholesterol by GCase, rendering not only XylChol, but also di-xylosyl-cholesterol and even small amounts of tri-xylosyl-cholesterol (Xyl_2Chol and Xyl_3Chol, respectively). Cells and tissues were found to contain low levels of XylChol. Subsequent investigations indicated that GBA2 plays no role in the metabolism (formation of degradation) of xylosylated lipids. Cells when exposed to 4-MU-β-Xyl produce XylChol in an entirely GCase-dependent manner. This reaction is favored during intralysosomal cholesterol accumulation as induced with the agent U88666A. Formation of XylChol

also occurs in cells incubated with the plant cyanidin 3-D-xyloside occurring in berries. Our subsequent studies revealed the presence of xylosylated ceramide (XylCer) in cells and tissues. This lipid is apparently synthesized by glucosylceramide synthase (GCS) using UDP-xylose as sugar donor. The same enzyme doesn't synthesize XylChol. Our findings on the unexpected existence of xylosylated lipids and their metabolism by glucocerebrosidase are discussed in relation to Gaucher disease.

Results

Cleavage of 4-methylumbelliferyl-β-D-xylose by GCase.

We first compared the ability of pure recombinant hGCase to cleave 4-MU-β-Xyl and 4-MU-β-Glc. The enzyme releases fluorescent 4-MU from both substrates, but the noted activity towards 4-MU-β-Xyl is around 70-fold lower as the result of a higher Km and lower Vmax (Table 1). The activity of GCase towards both substrates shows a similar pH optimum (Figure 1A) and stimulation by taurocholate (Figure 1B). The stimulatory effect of recombinantly produced saposin C on GCase-mediated cleavage of 4-MU-β-Glc and 4-MU-β-Xyl is comparable (Figure 1C). The kcat//Km of recombinant GCase is about 40-fold higher for 4-MU-β-Glc than 4-MU-β-Xyl (Table 1). The retaining β-glucosidase GCase employs the double displacement mechanism for catalysis with E340 as nucleophile and E325 as acid/base [16]. Blocking glutamate E340 by covalent linkage of the suicide inhibitor cyclophellitol abolishes activity of GCase [17]. The activity of GCase towards 4-MU-β-Glc and 4-MU-β-Xyl substrates was found to be both inhibited by pre-incubation for 90 minutes followed by an activity assay with the substrates for 60 minutes. The slightly higher apparent

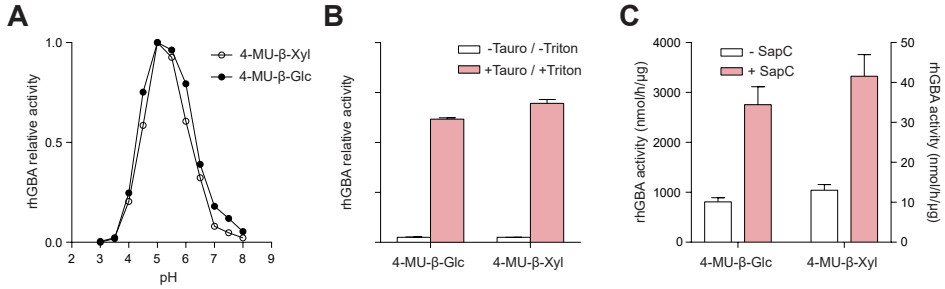

Figure 1: Cleavage of 4-MU-β-Glc and 4-MU-β-Xyl by recombinant hGCase. A. pH optimum of 4-MU release by GCase from 4-MU-β-Glc (closed circles) and 4-MU-β-Xyl (open circles). B. Stimulation by 0.2 % (w/v) taurocholate of 4-MU release from the substrates 4-MU-β-Glc (left) and 4-MU-β-Xyl (right). Expressed as 100 % is the activity measured in the absence of taurocholate at pH 5.2 with 0.1% (v/v) Triton X-100. C. Stimulation of 4-MU release from the substrates 4-MU-β-Glc (left axis) and 4-MU-β-Xyl (right axis) by recombinant saposin C at pH 4.5 in the presence of phosphatidylserine.

Table 1: Kinetic parameters hGCase

hGCase	4-MU-β-Glc	4-MU-β-Xyl
Km (mM)	0.76 ± 0.06	5.24 ± 1.04
Vmax (nmol/h.mg)	1.23 ± 0.03 x 106	1.88 ± 0.3 x 105
Kcat/Km (mM/s-1)	25.03	0.55
IC50 cyclophellitol (μM)	0.085 ± 0.002	0.061 ± 0.002
IC50 D-xylo-cyclophellitol (μM)	10.16 ± 1.03	6.41 ± 0.47

IC50 observed with 4-MU-β-Glc (85 nM) than with 4-MU-β-Xyl (61 nM) is likely explained by the greater protection against irreversible inhibition of GCase by the β-D-Glucose substrate. Recently a xylose analogue of cyclophellitol was synthesized [18]. It was observed that GCase is also irreversibly inactivated by D-Xylo-cyclophellitol, although with lower affinity than cyclophellitol (Table 1). Again, the apparent IC50 determined with 4-MU-β-Glc (10.16 μM) is slightly higher than with 4-MU-β-Xyl substrate (6.41 μM), presumably due to better protection of GCase against irreversible inhibition by the presence of 4-MU-β-Glc.

Transxylosidase activity of GCase.

We investigated recombinant GCase with respect to transxylosidase activity. For this, the enzyme was incubated for 16 hours with 4-MU-β-Glc or 4-MU-β-Xyl as donor and fluorescent 25-NBD-cholesterol as acceptor and next the products were analyzed by HPTLC and fluorescence scanning. Formation of fluorescent sterol metabolites occurred with both donors (Figure 2A). With 4-MU-β-Glc, glucosylated 25-NBD-cholesterol is formed as earlier described [10]. With 4-MU-β-Xyl, two novel fluorescent metabolites were detected, presumed to be mono- and di-xylosylated 25-NBD-cholesterol (Figure 2A).

Next, we used natural cholesterol as acceptor in the same assay with 4-MU-β-Xyl as donor and the formed products were analyzed by LC-MS/MS. In this way, formation of XylChol, Xyl_2Chol, and traces of Xyl_3Chol was detected (Figure 2B). In sharp contrast, incubation of GCase and cholesterol with 4-MU-β-Glc only renders GlcChol as product (Figure 2C).

Time dependence of glycosidase and transglycosidase activities of GCase.

GCase and cholesterol were incubated with 4-MU-β-Glc or 4-MU-β-Xyl at 37 ˚C for different time periods. The release of 4-MU and formation of glycosylated products was determined. The formed GlcChol was already maximal after an incubation of 30 min and subsequently declined with time (Figure 2C). This suggests that the formed GlcChol is subject to subsequent hydrolysis by GCase. In sharp contrast, XylChol showed no prominent reduction over time, and Xyl_2Chol was formed after a lag period (Figure 2D). This suggests

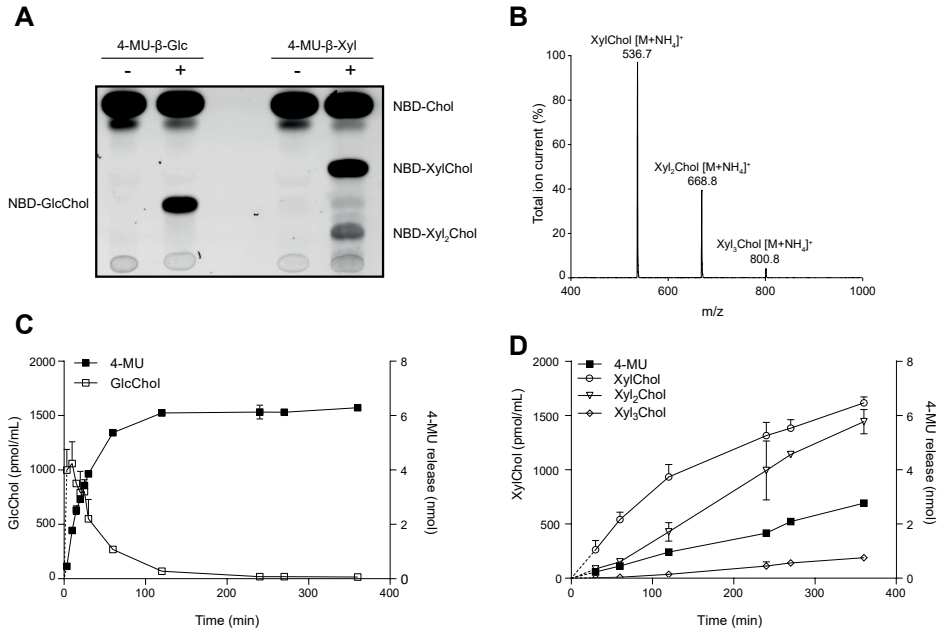

Figure 2: Transxylosylation and transglucosylation of cholesterol by GCase. A. HPTLC analysis of fluorescent products formed from 25-NBD-cholesterol following incubation with rGCase in the presence of 4-MU-β-Glc or 4-MU-β-Xyl for 16h. B. LC-MS/MS analysis of products formed during 1h incubation of rGCase, cholesterol and 4-MU-β-Xyl. C. Release of 4-MU from 4-MU-β-Glc and concomitant formation of glucosylated cholesterol in time. D. Release of 4-MU from 4-MU-β-Xyl and concomitant formation of xylosylated cholesterol in time. rGCase was incubated at pH 5.2 in the presence of taurocholate and Triton X-100 with 3.7 mM 4-MU-substrates for indicated times.

that XylChol is hardly hydrolyzed and acts as acceptor for further xylosylation. This process continues with Xyl_2Chol acting as acceptor rendering Xyl_3Chol (Figure 2D). A comparison of the release of 4-MU with concomitant formation of glycosylated sterol indicates that GCase shows considerably higher net transxylosylation than transglucosylation (Figure 2). We next studied the outcome of the incubation of GCase and cholesterol with 4-MU-β-Xyl (3 h) followed by 4-MU-β-Glc (1 h). Formation of GlcXylChol (with m/z 698.5 > 369.3) was demonstrable at these conditions, again pointing to XylChol acting as excellent acceptor in glycosylation reaction (Supplemental Table 2).

Time dependence of glycosidase and transglycosidase activities of GCase.

GCase and cholesterol were incubated with 4-MU-β-Glc or 4-MU-β-Xyl at 37 ˚C for different time periods. The release of 4-MU and formation of glycosylated products was determined. The formed GlcChol was already maximal after an incubation of 30 min and subsequently declined with time (Figure 2C). This suggests that the formed GlcChol is subject to subsequent

hydrolysis by GCase. In sharp contrast, XylChol showed no prominent reduction over time, and Xyl_2Chol was formed after a lag period (Figure 2D). This suggests that XylChol is hardly hydrolyzed and acts as acceptor for further xylosylation. This process continues with Xyl_2Chol acting as acceptor rendering Xyl_3Chol (Figure 2D). A comparison of the release of 4-MU with concomitant formation of glycosylated sterol indicates that GCase shows considerably higher net transxylosylation than transglucosylation (Figure 2). We next studied the outcome of the incubation of GCase and cholesterol with 4-MU-β-Xyl (3 h) followed by 4-MU-β-Glc (1 h). Formation of GlcXylChol (with m/z 698.5 > 369.3) was demonstrable at these conditions, again pointing to XylChol acting as excellent acceptor in glycosylation reaction (Data not shown).

In vivo *formation of xylosylated cholesterol.*

To substantiate our *in vitro* findings, potential transxylosylation by cultured RAW264.7 cells exposed to 3.7 mM 4-MU-β-Xyl was investigated. Cells were

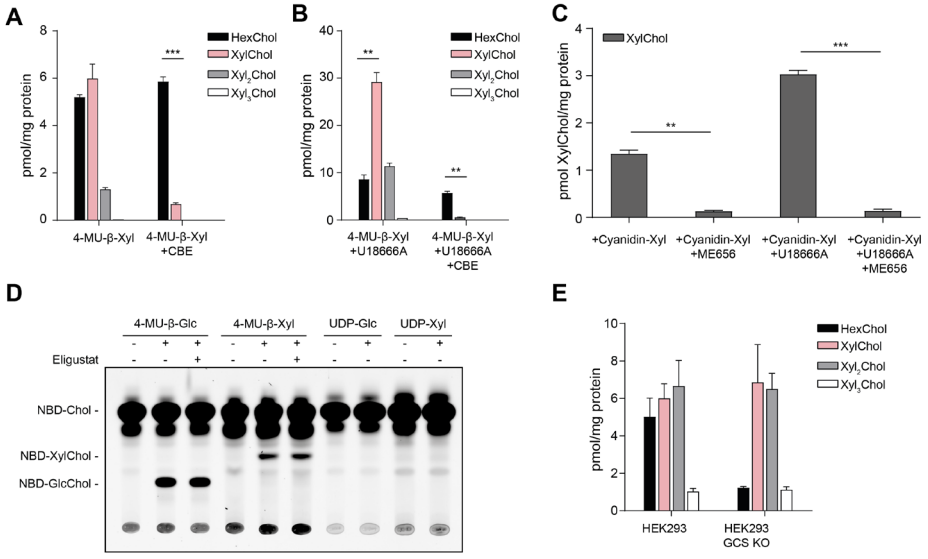

Figure 3: Formation of xylosylated cholesterols. A. LC-MS/MS detection of formed XylChol and HexChol (GlcChol or GalChol) in RAW264.7 cells incubated with 3.7 mM 4-MU-β-Xyl for 24 hours in the presence/absence of CBE, n=3 technical replicates and $p<0.05$. B. Idem in the presence of 10 μM U18666A. C. LC-MS/MS detection of formed xylosylated cholesterol in RAW264.7 cells incubated with 3.7 mM cyanidin 3-D-xyloside for 24 hours in the presence/absence of U18666A with/without GCase inhibitor ME656, n=2 technical replicates and $p<0.05$. D. HPTLC of in vitro formation of xylosylated cholesterols by HeLa cell lysate using NBD-Chol as acceptor and 4-MU-Glc, 4-MU-Xyl, UDP-Glc and UDP-Xyl as (potential) sugar donors in the prescence/absence of GCS inhibitor Eligustat. E. LC-MS/MS detection of formed xylosylated and glucosylated cholesterols in HEK293 and HEK293 GCS KO cells exposed to 3.7 mM 4-MU-β-Xyl and U18666A for 24 hours, n=3 technical replicates and $p<0.05$.

incubated with or without the irreversible GCase inhibitor conduritol B-epoxide (CBE) either in the absence (Figure 3A) or presence of 10 μM U18666A (Figure 3B) to induce lysosomal accumulation of cholesterol [10]. Formation of XylChol, Xyl_2Chol and Xyl_3Chol was detected by LC-MS/MS. The levels of xylosylated cholesterols were markedly increased by the exposure of cells to U18666A and prohibited by prior inhibition of GCase with CBE (Figure 3A and 3B). Several β-xylosidic compounds are known to be produced by plants and their uptake via food is likely [19, 20]. We therefore investigated whether cyanidin 3-D-xyloside from berries (Supplemental figure 3) can act as sugar donor in cellular formation of XylChol. For this purpose, RAW264.7 cells were incubated with cyanidin 3-D-xyloside for 24 hours and the formation of XylChol was monitored. Indeed, xylosylated cholesterol was formed by the exposed cells in GCase-dependent manner, as indicated by lack of its formation upon GCase inactivation by GCase specific inhibitor ME656 (Figure 3C). Addition of U18666A to the cells during incubation resulted in a little increase of the formed XylChol (Figure 3C). We next tested the possible involvement of UDP-glucose dependent GCS [21, 22]. Lack of involvement of GCS in the synthesis of XylChol was confirmed with an *in vitro* GCS assay by HPTLC (Figure 3D). Additionally, HEK cells made deficient in GCS by CRISPR-Cas9 produced XylChol on a par to corresponding cells when exposed to 4-MU-β-Xyl and U18666A (Figure 3E).

Specificity of transxylosylation.

We studied potential transxylosylation by the two other human retaining β-glucosidases, GBA2 and GBA3. We earlier noticed that GBA2, but not GBA3, can mediate transfer of the glucosyl moiety from 4-MU-β-D-Glc to cholesterol or ceramide [10]. While this finding was recapitulated (Supplemental figure 4), concomitantly no xylosylation by GBA2 was detectable consistent with GBA2's inability to hydrolyze 4-MU-β-D-Xyl [6]. However, GBA3, albeit less prominent than GCase, is able to hydrolyze 4-MU-β-Xyl as well as to transxylosylate cholesterol (Supplemental figure 4).

Table 2: Catalytic features of mutant GCase enzymes. Relative enzymatic activities in lysates of fibroblasts from GD patients incubated with 4-MU-Glc or 4-MU-Xyl to determine glucosidase and xylosidase activity. Cholesterol was added for trans activity determination. n=2 and values are expressed ± SD.

	Ratio	pmol/nmol	
Mutation	**Xylosidase /Glucosidase**	**Transglucosylation /Glucosidase**	**Transxylosylation /Glucosidase**
Control	0.035 ± 0.007	0.654 ± 0.076	0.044 ± 0.006
N370S	0.018 ± 0.001	0.391 ± 0.081	0.029 ± 0.012
L444P	0.028 ± 0.000	0.571 ± 0.066	0.044 ± 0.004
D409H	0.028 ± 0.004	0.182 ± 0.071	0.030 ± 0.001

β-Xylosidase and transxylosidase activities of mutant glucocerebrosidase of Gaucher disease patients.

Mutant forms of *GBA* commonly encountered in GD patients were compared to rGCase enzyme activity by using control and GD patient fibroblasts homozygous for N370S, L444P and D409H mutations in GCase. Cell lysates were incubated with either 4-MU-Glc or 4-MU-Xyl to determine their glucosidase and xylosidase activity by measuring the 4-MU release. Lysates were also incubated with 4-MU-Glc and 4-MU-Xyl concurrently with cholesterol as acceptor, followed by GlcChol and XylChol measurement (Table 2). These analyses showed a small reduction in xylosidase/glucosidase ratio in N370S compared to the control. Additionally we found a minor reduction in transglucosylation/glucosidase activity in GD fibroblasts with a D409H mutation compared to control.

Natural occurrence of xylosylated cholesterol.

We investigated next the presence of XylChol in cells and tissues. For this purpose, XylChol was synthesized to be used as internal standard in LC-MS/MS based quantitation of this lipid in materials. Figure 4A shows XylChol detection in fibroblast, HeLa, HEK293T and RAW264.7 cells as well as in human spleen and mouse liver. The XylChol levels are relatively low as compared to those of HexChol (GlcChol or GalChol), although the ratio HexChol:XylChol differs per cell type and tissue (data not shown). In cells, XylChol levels are on average 130 fold less than those of HexChol. In liver relatively much lower amounts of XylChol were noted. However, relatively more XylChol was detected in liver of $Npc1^{-/-}$ mice, earlier found to also contain high levels of GlcChol [10]. Of note, in spleens of type 1 GD patients reduced XylChol concentrations were observed.

Xylosylated ceramide as a potential xylose donor for GCase.

In search for an endogenous xylose donor in the generation of XylChol, the occurrence of xylosylated ceramide (XylCer) was examined. For this purpose, a LC-MS/MS based quantitation was developed, based on microwave-assisted deacylation to xylosylated sphingosine of which a standard was synthesized. We measured XylCer levels in the same materials previously used for XylChol measurement (Figure 4B). Of note, XylCer is increased in GD spleen, whereas XylChol is reduced in the patient's organ (Figure 4A). Apparently, GCase does not degrade XylChol but synthetizes it. On the other hand, GCase can degrade XylCer and thus might use XylCer as sugar donor in the formation of XylChol. To test whether XylCer is a suitable sugar donor in formation of XylChol we generated XylCer and next incubated it with cholesterol and recombinant GCase. Formation of XylChol was detected by LC-MS/MS (Figure 5A), confirming XylCer might act as a sugar donor.

Glucosylceramide synthase synthesizing cylosylated ceramide.

Our discovery of XylCer stimulated the search for a XylCer generating enzyme. As candidate the enzyme GCS was tested. First, an *in vitro* assay with UDP-Xyl as donor and NBD C6-ceramide as acceptor incubated for 16 h with lysate of HEK293T cells led to formation NBD-XylCer and possibly NBD-Xyl$_2$Cer was detected (Figure 5B). The same assay was performed with ceramide d18.1/18.1 as acceptor and resulted likewise in formation of XylCer, as detected by LC-MS/MS (Figure 5C). Lysates of cells lacking GCS were found to be unable to generate XylCer. Upon overexpression of GCS in the GCS KO

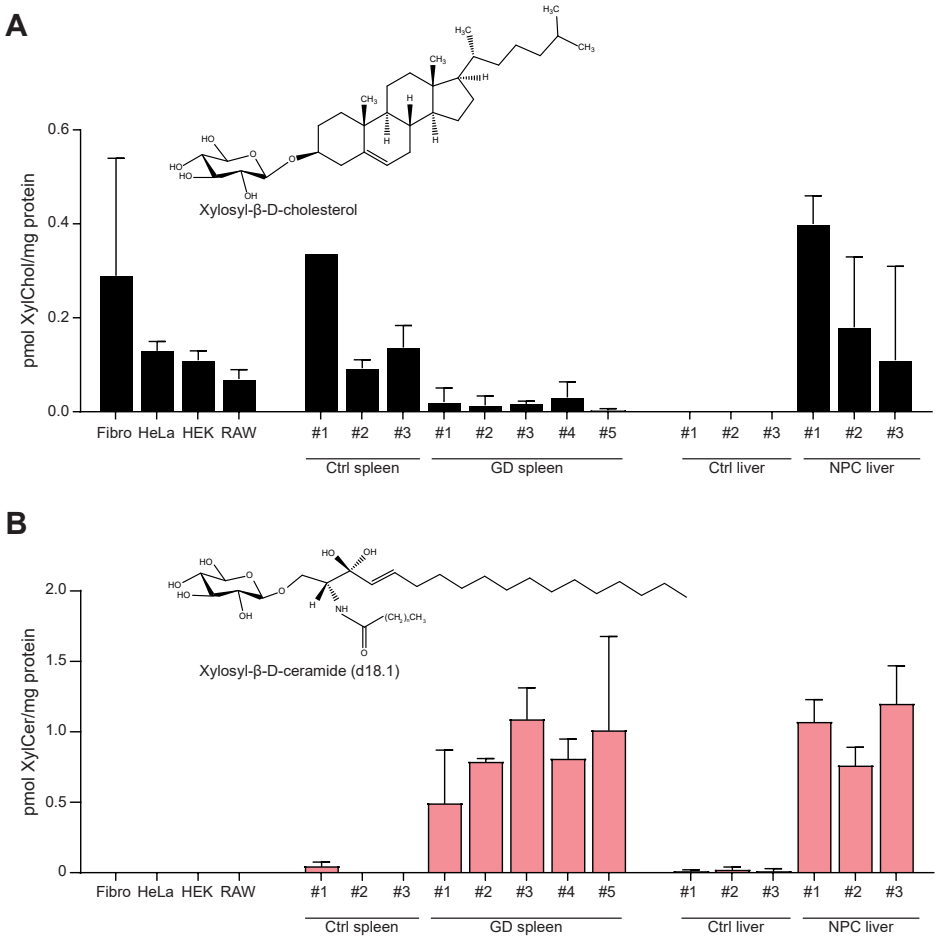

Figure 4: Levels of xylosylated cholesterol and ceramide found in cells and organs. A. LC-MS/MS analysis of XylChol occurrence in Fibroblasts, HeLa, HEK293, RAW264.7 cells, human control spleens, human GD spleens, mouse control livers and mouse NPC livers. B. LC-MS/MS analysis of XylCer occurrence in Fibroblasts, HeLa, HEK293, RAW264.7 cells, human control spleens, human GD spleens, mouse control livers and mouse NPC livers. Error bars are standard deviation of technical duplicates.

cells corresponding the cell lysates were regained the ability to produce XylCer (Figure 5C). This novel function of GCS was further confirmed using lysates of the GCS-deficient GM95 cells and the parental GCS-competent MEB4 B16 cells incubated with UDP-Xyl and ceramide d18.1/18.1, where only the MEB4 cells showed formation of XylCer (Figure 5D).

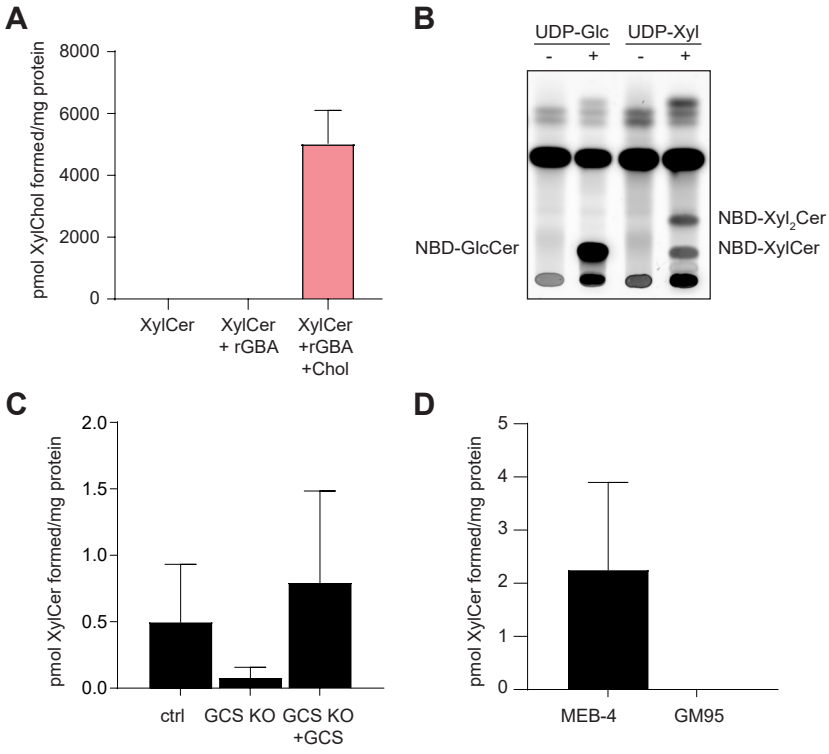

Figure 5: XylCer is a donor for GCase to transxylosylate cholesterol and can be synthesized by GCS. A.XylCer (formed by incubation 4-MU-Xyl, Ceramide d18.1/18.1 and rGCase at pH 5.2) was incubated with rGCase and cholesterol at pH 5.2 for 18 hours at 37°C. The figure depicts LC-MS/MS measurement of formed XylChol. Errorbars represent standard deviation of technical duplicate. B. HPTLC analysis of formation of glycosylated NBD C6-ceramide by GCS with UDP-Glc or UDP-Xyl as donor. C. LC-MS/MS analysis of formed glycosylated ceramide after incubation of cell lysates of HeLa, HeLa GCS KO or HeLa GCS KO with a reintegrated overexpression of GCS with UDP-Glc or UDP-Xyl and ceramide d18.1/18.1. Incubations were 16 hours, errorbars represent standard deviation n=2. D. LC-MS/MS analysis of formed glycosylated ceramide after incubation of mouse fibroblast lysates with UDP-Glc or UDP-Xyl and ceramide d18.1/18.1. Incubations were 16 hours, errorbars represent standard deviation n=2.

Discussion

Our present investigation reveals an intriguing novel catalytic feature of human GCase, the lysosomal glucocerebrosidase. First, we noted that GCase cleaves *in vitro* besides 4-MU-β-Glc also 4-MU-β-Xyl. Moreover, the enzyme uses both substrates as sugar donors in transglycosylation of cholesterol molecules. Next, we observed the generation of xylosylated cholesterol in living cells exposed to 4-MU-β-Xyl. Induction of lysosomal cholesterol accumulation in cells with U18666A increases formation of xylosylated cholesterols, a reaction prohibited by inactivation of GCase with the irreversible inhibitor CBE. Remarkably, both *in vitro* and *in vivo*, GCase may even produce di-xylosyl-cholesterol using 4-MU-β-Xyl as sugar donor, a repetitive transglucosylation not seen with 4-MU-β-Glc as sugar donor [10]. The affinity of GCase for 4-MU-β-Glc as substrate for cleavage is higher than that for 4-MU-β-Xyl. Likewise, XylChol is a much poorer substrate for hydrolysis by GCase than GlcChol. Following exposure of GCase to cholesterol and 4-MU-β-Xyl, the concentration of XylChol steadily builds up and it starts to act as acceptor in a second round of transxylosylation, rendering Xyl_2Chol. Incubation of GCase and cholesterol with a mixture of 4-MU-β-Xyl and 4-MU-β-Glc leads to formation of GlcXylChol, further highlighting the suitability of XylChol as acceptor in transglycosylation by GCase. Of note, Aerts and co-workers earlier noted also relative higher net transxylosylase than transglucosylase efficiency of a β-D-glucosidase from Stachybotrys atra [19], quite comparable to our findings with GCase. We modelled XylChol in the crystal structure of human GCase (data not shown). Indeed, XylChol can be positioned in the pocket as acceptor for another round of transglycosylation. Obviously real life crystallography experiments with soaked lipids in the crystal will be required to obtain conclusive data and further insight.

The possible physiological relevance of transxylosylation by GCase warrants discussion. Mass spectrometry shows the presence of significant amounts of XylChol in liver of Npc1-/- mice. XylChol was also detected in low quantities in cells, liver and spleen. Interestingly, in type 1 GD spleens XylChol levels were clearly reduced as compared to control spleens. This finding substantiates the notion that GCase is largely responsible for formation of XylChol and the same enzyme is only poorly able to degrade it, in contrast to its ability to hydrolyze 4-MU-β-xyloside. Of interest, the β-glucosidase GBA2 shown earlier to be a potent transglucosidase generating GlcChol has no significant activity towards β-xyloside substrates. Apparently the pendant CH2OH group in glucoside substrates contributes crucially to the interaction of substrate with GBA2. The importance of the presence of the additional CH2OH group in glucose is also suggested by the much lower affinity of GBA2 for the inhibitor conduritol-B-epoxide as compared to cyclophellitol (with the pendant CH2OH group) [23]. In

contrast to GBA2, the enzyme GBA3, a cytosolic broad-specificity glycosidase implicated in metabolism of xenophobic glycosides [24], shows xylosidase and transxylosidase activity in *in vitro* experiments. The contribution of this enzyme in metabolism of xylosides is presently still unclear.

Our discovery of catalytic activities of GCase (β-glucosidase, β-xylosidase, transglucosylase and transxylosylase) prompted us to look into the possibility that specific mutant forms of GCase as occurring in GD patients may have selective abnormalities in one of the activities. Analyzing patient fibroblast with common GD mutations N370S, L444P and D409H GCase did not point to specific abnormalities in one of the catalytic activities as tested with 4-MU-Glc and 4-MU-Xyl as substrates and cholesterol as acceptor. We were particularly interested in any abnormalities in catalytic features of D409H GCase since this mutation is associated with an unique symptomatology involving valve calcification [25-27]. Although we detected no specific abnormalities for this particular mutant enzyme it nevertheless remains of interest to study in biopsy materials of GD patients with D409H patients the presence of abnormal β-xylosides.

In the course of our investigation a key question concerned the nature of physiological xyloside donors. Several β-xylosidic compounds are known to be produced by plants and their uptake via food is a priori not excluded [19, 20]. We did show the ability of *in vivo* formation of XylChol in cells when incubated with cyanidin 3-D-xyloside, which is found in plums and berries. Making it likely there might be other plant originated β-xylosides that are suitable donors for GCase-mediated formation of xylosylated sterols. An alternative endogenous donor of β-D-xylosyl moieties might be degradation products of proteoglycans. During their lysosomal degradation β-D-xylosyl-peptides are formed. Our investigation also revealed another, somewhat unexpected, candidate: xylosylated ceramide. Actually, the occurrence of XylCer has been previously reported in the salt gland of the herring gull [28]. Our investigation demonstrated the presence of XylCer in human and mouse materials, although at very low levels as compared to GlcCer. Additionally, XylCer can serve as a donor for transxylosylation of cholesterol by GCase. Extension of these findings resulted in the finding of a novel function of GCS, that is able to use UDP-Xyl to form XylCer, although with much lower affinity than UDP-Glc. XylCer was found to be elevated in GD spleen, consistent with this lipid being a substrate for GCase and possible sugar donor in transylosylation mediated by the lysosomal enzyme. The physiological relevance of the relatively tiny amounts of XylCer is presently enigmatic. It requires further studies to establish whether exogenous β-xylosides of plant origin or endogenous β-xylosides (β-D-xylosyl-peptides or XylCer) acts donors in formation of XylChol.

In conclusion, human GCase is more versatile in catalysis as hitherto considered. Investigation of the (patho)physiological relevance of various reactions catalyzed by GCase and xylosylated lipids is needed to further complete understanding of the full symptomatology of Gaucher disease [7, 8] and other conditions for which abnormal GCase imposes a risk such as multiple myeloma and α-synucleinopathies like Parkinsonism and Lewy-body dementia [29].

Materials and Methods

Materials. 25-[N-[(7-nitro-2-1,3-benzoxadiazol-4-yl)methyl]amino]-27-norcholesterol (25-NBD-cholesterol) were purchased from Avanti Polar Lipids (Alabaster, AL, USA). (6-((N-(7-Nitrobenz-2-Oxa-1,3-Diazol-4-yl)amino) hexanoyl)Sphingosine) (NBD C6-Ceramide) was purchased from Invitrogen (Waltham, MA, USA). 4-methylumbelliferyl β-D-glucose (4-MU-Glc) and 4-methylumbelliferyl β-D-xylose (4-MU-Xyl) were purchased from Glycosynth™ (Winwick Quay Warrington, Cheshire, England). Cyanidin 3-Xyloside was obtained from Toronto Research Chemicals (Martin Ross Ave, North York, Canada). Uridine diphosphate glucose (UDP-Glc), Cholesterol, cholesterol trafficking inhibitor U18666A, 1-O-cholesteryl-β-D-glucose (β-cholesteryl glucose, β-GlcChol) and ammonium formate (LC-MS quality) were from Sigma-Aldrich (St Louis, MO, USA). Uridine diphospho- alpha-D-xylopyranoside (UDP-Xyl) was purchased from CarboSource Services (Riverbend Rd, Athens, USA - Supported in part by Grant #DE-FG02-93ER20097). GCase inhibitor Conduritol-β-epoxide (D, L-1,2-anhydro-myo-inositol; CBE) was from Enzo Life Sciences Inc. (Farmingdale, NY, USA), GCase inhibitor cyclophellitol, GBA2 inhibitor N-(5-adamantane-1-yl-methoxy-pentyl)-deoxynojirimycin (AMP-DNM), GBA3 inhibitor α-1-C-nonyl-DIc (anDIX) and 1-O-cholesteryl-β-D-xylose (XylChol) were synthesized at Leiden Institute of Chemistry (Leiden, The Netherlands) [24, 30]. Cerezyme®, a recombinant human GCase was obtained from Genzyme (Genzyme Nederland, Naarden, The Netherlands). LC-MS–grade methanol, 2-propanol, water, and HPLC-grade chloroform was purchased from Biosolve. D-xylo-cyclophellitol was synthesized as reported earlier [18].

Collection of Niemann-Pick type C mouse livers and GD patient spleens. Livers from Npc1-/- mice (Npc1nih), along with wild-type littermates (Npc1+/+), were collected in a previous study [10]. All human spleens were obtained either as surgical specimens during therapeutic splenectomy or at autopsy. The phenotype of the subjects was established by clinical examination. All organs were stored at -80 °C. Later, homogenates were made from the frozen material in water.

Cloning and expression of cDNAs encoding GBA2, GBA3 and GCS. The design of cloning primers was based on NCBI reference sequences NM_020944.2 for human GBA2, and NM_020973.3 for human GBA3 as described previously [10]. Glucosylceramide synthase (GCS) in HEK293 cells was knocked-down by the CRISPR/Cas9 system [31]. The coding sequence of GCS was amplified by PCR (using the following oligonucleotides: sense. 5'-GGGGACAAGTTTG TACAAAAAAGCAGGCTACCACCATGGCGCTGCTGGACCTG-3'and antisense '-GGGGACCACTTTGTACAAGAAAGCTGGGTCTTATACATCTAGGATTTCCTCTG-3') and cloned into pDNOR-221 and sub cloned in pcDNA3.1-Zeo via Gateway cloning system (Invitrogen). Correctness of the construct was verified by sequencing. HEK293 cells were obtained from the "American Type Culture Collection" and cultured in Iscove's modified Dulbecco's medium with 5% FBS and penicillin/streptomycin under 5% CO2 at 37°C. For transfection cells were seeded at 75% confluence in 6-well plates and transfected using PEI Transfection reagent (Polysciences Inc, Valley Rd, Warrington, USA) according to the manufacturer's instructions, at a PEI:DNA ratio of 3:1.

Culturing and collection of GD fibroblasts. Control and GD patient fibroblasts homozygous for N370S, L444P and D409H mutations in *GBA* were cultured in HAMF12-DMEM medium supplied with 10% FBS and penicillin/streptomycin at 37°C under 7% CO2. Fibroblasts were collected by trypsinization followed by 3x washing with ice cold PBS. Cells were homogenized in 25mM potassium phosphate buffer pH 6.5 supplemented with 0.1 % (v/v) Triton X-100 by sonication on ice.

In vitro *assays with fluorogenic 4-methylumbelliferyl-β-D-glycosides.* Enzymatic activity of GCase was measured with 3.7 mM 4-MU-β-Glc or 4-MU-β-Xyl, dissolved in 150 mM McIlvaine buffer (pH 5.2 supplemented with 0.2 % (w/v) sodium taurocholate, 0.1 % (v/v) Triton X-100) and 0.1 % (w/v) BSA) [32]. The reaction was stopped with NaOH-glycine (pH 10.3), and fluorescence was measured with a fluorimeter LS-55 (Perkin-Elmer, Beaconsfield, UK) at λex 366 nm and λex 445 nm. Enzymatic activity of GBA2 was measured in lysates of cells overexpressing the enzyme using the same conditions as above but without the presence of detergents and at pH 5.8. Enzymatic activity of GBA3 was measured in the absence of detergents in 100mM HEPES buffer at pH 7.0 [24]. Stimulation of GCase activity by the activator protein saposin C, produced recombinantly in *E. coli* [33], was monitored with 3.7 mM 4-MU-β-Glc as substrate in 150 mM McIlvaine buffer pH 4.5 containing 0.1 % (w/v) BSA and 0.4 mg/mL phosphatidylserine [34].

In vitro *assay of transglycosidase activity with fluorescent 25-NBD-cholesterol as acceptor.* Recombinant GCase and lysates of HEK293 cells overexpressing GBA2 and GBA3 were used to determine transglycosidase activity of each enzyme. The assays were performed as described earlier [10]. First, lysates overexpressing GBA2, or GBA3 were pre-incubated with 5 µM CBE for 20 min (samples containing diluted recombinant GCase were pre-incubated in the absence of CBE). To each of the samples the appropriate buffer containing 4-MU-Xyl or 4-MU-Glc was added for a final donor concentration of 3 mM and a final concentration of 40 µM 25-NBD-cholesterol as acceptor. Transglycosidase activity of GBA2 overexpressing cells was measured in a 150 mM McIlvaine buffer pH 5.8 and the assay for recombinant GCase was done in a 150 mM McIlvaine buffer pH 5.2 containing 0.1% BSA, 0.1% Triton X-100 and 0.2% sodium taurocholate. For GBA3 the assay contained 100 mM HEPES buffer, pH 7.0. The reaction was terminated by addition of chloroform/methanol (1:1, v/v) and lipids were extracted according to Bligh and Dyer [35]. Thereafter lipids were separated by thin layer chromatography on HPTLC silica gel 60 plates (Merck, Darmstadt, Germany) using chloroform/methanol (85:15, v/v) as eluent followed by detection of NBD-labelled lipids using a Typhoon Variable Mode Imager (GE Healthcare Bio-Science Corp., Piscataway, NJ, USA) [6].

In vitro *assay of GCS activity with fluorescent NBD C6-ceramide as acceptor.* HeLa, HeLa GCS KO and HeLa GCS KO with overexpression of GCS cell were homogenized in 100mM potassium phosphate buffer pH 7.5 supplemented with 4mM MgCl2 by sonication on ice. These homogenates were incubated with 35µM NBD C6-ceramide and 10 mM of UDP-Glc or UDP-Xyl for 16 hours. Lipids were extracted, separated and visualized as described above.

In vitro *assay of transglycosidase activity with cholesterol as acceptor.* Assays with natural cholesterol or ceramide d18:1/18:1 as acceptor were performed exactly as described in the sections above and the subsequent analysis of products was performed by LC-MS/MS as described in the section below. In brief for cholesterol: pure recombinant GCase was incubated at 37 ˚C with 32 µM cholesterol and 3.0 mM 4-MU-β-Xyl or 4-MU-β-Glc in 150 mM McIlvaine buffer pH 5.2 containing 0.1% BSA, 0.1% Triton X-100 and 0.2% sodium taurocholate for the indicated time periods. In short for ceramide: 10mM of UDP-Glc or UDP-Xyl was incubated with 0.16 µM ceramide d18.1/18:1 for 16 hours. All the incubations were stopped by addition of chloroform/methanol (1:1, v/v) and lipids were extracted according to Bligh and Dyer.

Assays with cultured RAW264.7 and HEK293 cells. Experiments with cultured RAW264.7 and HEK293 cells exposed to 3.7 mM 4-MU-β-Xyl or cyanidin 3-D-xyloside in the medium, either in the absence or presence of U18666A

(10 µM), inducing lysosomal cholesterol accumulation, were performed as described earlier [10]. Lysosomal GCase was irreversibly inhibited by prior incubation of cells with 300 µM CBE or 20nM ME656. Cells were harvested and lipids extracted as earlier described [10].

Synthesis Xylosylated Cholesterol. A complete overview of the synthesis of β-cholesteryl xyloside can be found in the supplemental materials and methods.

LC-MS/MS analysis. A Waters Xevo-TQS micro instrument was used in all experiments. The instrument consisted of an UPLC system combined with a tandem quadruple mass spectrometer as mass analyzer. Data were analyzed with Masslynx 4.1 Software (Waters,Milford MA, USA). Tuning conditions for GlcChol, XylChol's, GlcXylChol's, GlcSph and XylSph in ES+ (electrospray positive) mode are presented in Supplemental Table 1. All lipids during this study were separated using an Acquity BEH C18 reversed-phase column (2.1x 50 mm, particle size 1.7 µm; Waters). The column temperature and the temperature of the auto sampler were kept at 23°C and 10°C respectively during the run. The flow rate was 0.250 mL/min and volume of injection 10µL.

Analysis of GlcChol, and XylChol by LC-MS/MS. For the identification of XylChol, the extracted sample was dried and dissolved in methanol. MS parents scan and daughters scan were performed (Figure 2). As for GlcChol [10], the most abundant species of XylChol are ammonium adducts, [M+NH4]+ and the product ion 369.3 represents the cholesterol part of the molecule after loss of the xylose moiety. Ammonium adducts of XylChol, Xyl_2Chol and Xyl_3Chol showed the transitions 536.5>369.3, 668.5>369.3 and 800.5>369.3 respectively. For Multiple Reaction Monitoring (MRM) the UPLC program was applied during 5.5 minutes consisting of 10% eluent A (2-propanol:H2O 90:10 (v/v) containing 10 mM ammonium formate) and 90% eluent B (methanol containing 10 mM ammonium formate) The divert valve of the mass spectrometer was programmed to discard the UPLC effluent before (0 to 0.8 min) and after (4.5 to 5.5 min) the elution of the analytes to prevent system contamination. The retention time of both GlcChol and the internal standard $^{13}C_6$-GlcChol was 1.36 min. XylChol's were either synthesized or generated *in vitro* by incubation of GCase with 4-MU-β-Xyl and cholesterol. The retention time of XylChol, Xyl_2Chol and Xyl_3Chol was 1.71 min, 1.49 min and 1.40 min respectively (Supplemental Figure 1). Lastly, plasma was spiked with pure XylChol (0-1000 pmol XylChol/mL of plasma), internal standard $^{13}C_6$-GlcChol was added and samples were extracted. The area from transition XylChol over the area from the transition of internal standard (the ratio) was plotted against the concentration of XylChol in the plasma samples. The limit of detection was 0.1 pmol/mL plasma with

a sinal-to-noise ratio of three and the limit of quantification was 10 pmol/mL pasma with a signal-to-noise ratio of ten. Calculation of the signal-to-noise ratio was done using the peak-to-peak method.

LC-MS/MS quantitation of GlcChol and XylChols produced in vitro. Following incubation of rGCase and cholesterol with either 4-MU-β-Glc or 4-MU-β-Xyl, lipids were extracted according to the method of Bligh and Dyer by addition of methanol, chloroform and water (1:1:0.9, v/v/v). The lower phase was taken to dryness in an Eppendorf concentrator. Isolated lipids were purified by water/butanol extraction (1:1, v/v). The upper phase (butanol phase) was dried and dissolved in methanol, sonicated in a bath sonicator and samples were analyzed by LC-MS.

LC-MS/MS quantitation of GlcChol and XylChol's in cultured cells and organs. Cells were homogenized in 25mM potassium phosphase buffer pH 6.5 containing 0.1% (v/v) triton, by sonication on ice. Livers and spleens were homogenized in water. Prior to extraction, ^{13}C-labelled GlcChol and ceramide d17.0/16.0 in methanol (both used as an internal standard) were added to the homogenate. Samples were then treated with methanol:chloroform (1:1, v/v) to precipitate the proteins, following the supernatant was further extracted as described above.

Analysis of GlcCer, and XylCer by LC-MS/MS. To measure GlcCer and XylCer, lipids were deacylated [36] after Bligh and Digher extraction with methanol, chloroform and 100mM formate buffer pH 3.0 (1:1:0.9, v/v/v). Next, sample was evaporated and purified by water/butanol extraction (1:1, v/v). The butanol phase was dried, the final sample dissolved in methanol and GlcSph and XylSph levels measured. GlcSph was analyzed as published previously [37]. For Xylsph identification the sample was introduced in the mass spectrometer using LC-MS/MS (from 0 to 6.5 min to the detector), using eluent A (H2O:formic acid 99.5/0.5 (v/v) containing 1 mM ammonium formate) and eluent B (methanol:formic acid 99.5/0.5 (v/v) containing 1 mM ammonium formate). A mobile phase gradient was used during the run: 0.00 min 0% B, 2.50 min 100% B, 6.00 min 100% B, 6.05 min 0% B and 6.50 min 0% B.
MS parents scan and daughters scan were performed (Supplemental figure 2). Single reaction monitoring of precursor -> fragment ions (m/z GlcSph 462.30 > 282.30 and XylSph 432.67 > 282.30) was used for quantification.

Protein determination. Protein was measured with the Pierce BCA Protein Assay kit (Thermo Scientific). Absorbance was measured in EL808 Ultra Microplate Reader (BIO-TEK Instruments Inc.) at 562 nm.

Statistical Analysis. Values in figures are presented as a mean ± S.D. Data were analyzed by unpaired Student's t-test or Mann-Whitney u-test. P values < 0.05 were considered significant. * P < 0.05, ** P < 0.01 and *** P < 0.001.

Supplemental Materials and Methods

Synthesis of β-cholesteryl xyloside (β-Xyl-Chol).

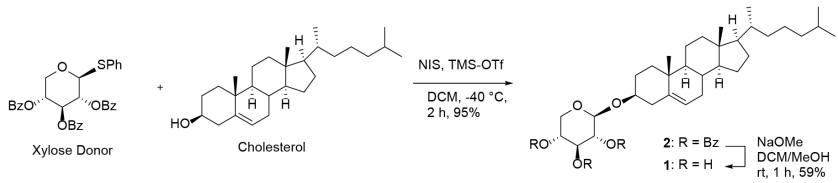

Unless stated otherwise, starting materials, reagents and solvents were purchased as high-grade commercial products from Sigma-Aldrich and were used without further purification. Dichloromethane (DCM) stored over 4 Å molecular sieves, which were dried in vacuo before use. Reactions were monitored by analytical thin-layer chromatography (TLC) using Merck aluminum sheets pre-coated with silica gel 60 with detection by UV absorption (254 nm) and by spraying with a solution of (NH4)6Mo7O24·H2O (25 g/L) and (NH4)4Ce(SO4)4·H2O (10 g/L) in 10% sulfuric acid followed by charring at ~150 ˚C or by spraying with an aqueous solution of KMnO4 (7%) and K2CO3 (2%) followed by charring at ~150 °C. Column chromatography was performed manually using either Baker or Screening Device silica gel 60 (0.04 - 0.063 mm), or with a Biotage Isolera™ flash purification system using silica gel cartridges (Screening devices SiliaSep HP, particle size 15-40 µm, 60A) in the indicated solvents. 1H NMR and ^{13}C NMR spectra were recorded on Bruker AV-500 (500/125 MHz) spectrometer in the given solvent. Chemical shifts are given in ppm relative to the chloroform, methanol, or dimethylsulfoxide residual solvent peak or tetramethylsilane (TMS) as internal standard. The following abbreviations are used to describe peak patterns when appropriate: s (singlet), d (doublet), t (triplet), q (quartet), qt (quintet), m (multiplet), br (broad), ar (aromatic), app (apparent). LC/MS analysis was performed on A Waters Acquity TM TQD instrument. The instrument consisted of a UPLC system combined with a tandem quadrupole mass spectrometer as mass analyzer using a BEH C18 reversed-phase column (2.1 × 50 mm, particle size 1.7 µm; Waters Corporation), by applying an isocratic elution of mobile phases, 2-propanol:water 90:10 (v/v) containing 10 mM ammonium formate (eluent A) and methanol containing 10 mM ammonium formate (eluent B).

β-cholesteryl xylosyl benzoate 2. (2S,3R,4S,5R)-2-(phenylthio)tetrahydro-2H-pyran-3,4,5-triyl tribenzoate donor1 (111 mg. 0.20 mmol) and cholesterol (62 mg, 167 mmol) were co evaporated in toluene (2x) and re-dissolved in 2 mL of DCM. 4Å molecular sieves were added and the mixture was stirred for 30 min at room temperature. Then the mixture was cooled to -40 °C and NIS (45 mg, 0.20 mmol) and TMS-OTf (42 µL, 0.23 mmol) were added. After stirring for 2 h at -40 °C the reaction was quenched with Et3N and warm up to room temperature. The mixture was diluted with DCM (30 mL) and aqueous 10% Na2S2O3 (20 mL). The extracted organic phase was then washed with brine, dried and purified by silica gel column chromatography (from pentane to pentane:EtOAc 9:1) to afford the protected β-cholesteryl xyloside 2 in 95% yield. 1H NMR (500 MHz, CDCl3): δ 7.99 (ddd, J = 7.1, 4.1, 1.2 Hz, 5H), 7.55 – 7.47 (m, 3H), 7.36 (q, J = 8.0 Hz, 6H), 5.76 (t, J = 7.4 Hz, 1H), 5.34 (dd, J = 7.5, 5.6 Hz, 1H), 5.29 – 5.27 (m, 1H), 4.95 (d, J = 5.6 Hz, 1H), 4.44 (dd, J = 12.1, 4.4 Hz, 1H), 3.68 (dd, J = 12.1, 7.3 Hz, 1H), 3.57 (tt, J = 11.3, 4.6 Hz, 1H), 2.46 – 2.33 (m, 1H), 2.27 (ddd, J = 13.3, 4.9, 2.2 Hz, 1H), 2.20 – 2.11 (m, 1H), 2.06 – 1.90 (m, 2H), 1.90 – 1.76 (m, 3H), 1.73 – 1.47 (m, 8H), 1.47 – 1.19 (m, 6H), 1.19 – 1.02 (m, 6H), 1.02 – 0.97 (m, 2H), 0.95 (s, 3H), 0.91 (d, J = 6.6 Hz, 3H), 0.87 (d, J = 2.2 Hz, 3H), 0.85 (d, J = 2.2 Hz, 3H), 0.66 (s, 3H). 13C NMR (126 MHz, CDCl3) δ 165.7, 165.6, 165.4, 140.5, 133.5, 133.3, 130.0, 129.6, 129.4, 129.4, 128.5, 122.2, 98.8, 79.0, 77.4, 77.2, 76.9, 70.9, 70.7, 69.5, 61.5, 56.9, 56.3, 50.3, 42.5, 39.9, 39.7, 38.8, 37.4, 36.9, 36.3, 35.9, 32.1, 32.0, 29.9, 29.7, 28.4, 28.3, 28.2, 24.4, 24.0, 23.0, 22.7, 21.2, 19.5, 18.9, 12.0.

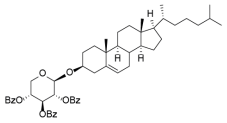

β-cholesteryl xyloside1. Intermediate 2 (63 mg, 0.076 mmol) was dissolved in a mixture of DCM/MeOH (1:2, v/v, 3 mL) and NaOMe (5.4 M in MeOH, 7.6 µL). After stirring for 1 h the reaction mixture was neutralized by addition of Et3N·HCl and purified by silica gel column chromatography (from DCM to DCM:MeOH 9:1), yielding the title compound cholesteryl-D-β-Xylopyranoside (β-Xyl-Chol) 1 as a white solid in 59% yield. 1H NMR (500 MHz, CDCl3): δ 5.37 (d, J = 5.1 Hz, 1H), 4.50 (d, J = 6.1 Hz, 1H), 4.05 (dd, J = 11.9, 4.4 Hz, 1H), 3.75 (dq, J = 8.0, 4.0 Hz, 1H), 3.65 – 3.53 (m, 2H), 3.47 – 3.40 (m, 1H), 3.36 (dd, J = 11.9, 8.1 Hz, 1H), 2.94 (s, 1H), 2.64 (d, J = 4.1 Hz, 1H), 2.42 – 2.34 (m, 2H), 2.23 (t, J = 12.5 Hz, 1H), 2.04 – 1.95 (m, 2H), 1.91 – 1.81 (m, 2H), 1.64 – 1.43 (m, 10H), 1.36 – 1.23 (m, 6H), 1.16 – 1.04 (m, 6H), 1.00 (s, 3H), 0.91 (d, J = 6.5 Hz, 3H), 0.87 (d, J = 2.3 Hz, 3H), 0.86 (d, J = 2.4 Hz, 3H), 0.67 (s, 3H). 13C NMR (126 MHz, CDCl3) δ 140.2, 122.5, 100.8, 78.7, 74.6, 72.5, 69.9, 64.3, 56.9, 56.3, 50.3, 42.5, 39.9, 39.7, 38.8, 37.4, 36.9, 36.3, 35.9, 32.1, 32.0, 29.8, 28.4, 28.2, 24.4, 24.0, 23.0, 22.7, 21.2, 19.5, 18.9, 12.0. LC-MS/MS: calcd. for [C32H54O5+NH3]+ 518.8; found 536.7.

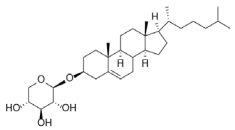

Supplemental data

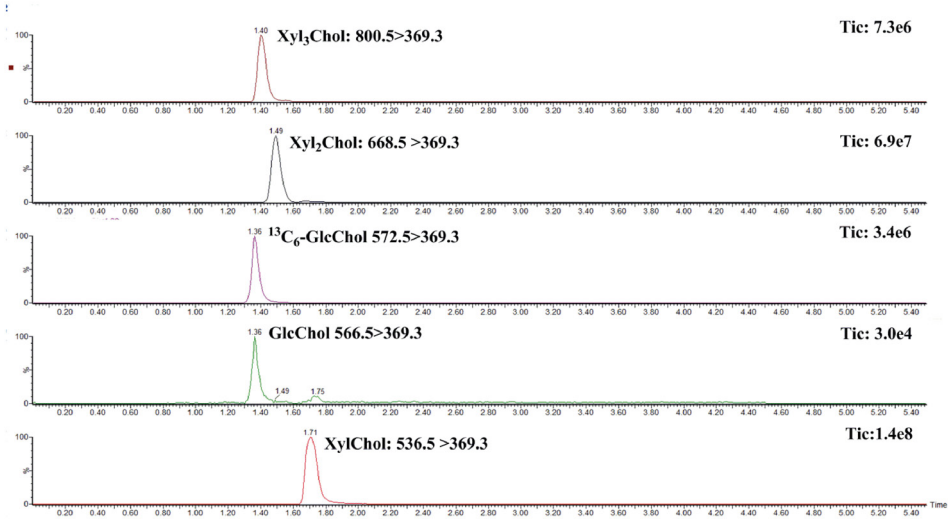

Supplemental Figure 1: Chromatogram of XylChol, Xyl_2Chol, Xyl_3Chol, GlcChol and $^{13}C_6$-GlcChol.

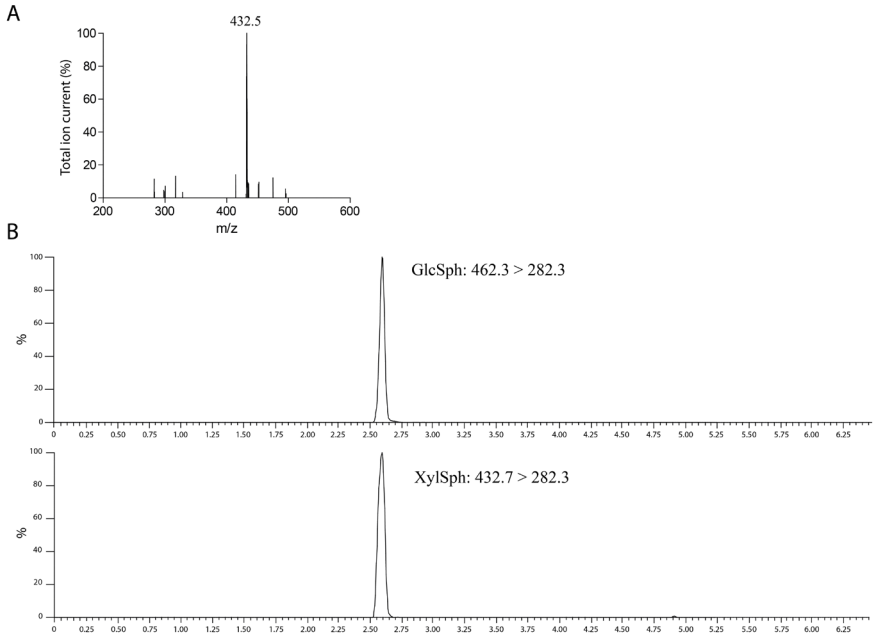

Supplemental Figure 2: A. MS/MS Fragmentation spectrum of parent scan XylSph B. Chromatogram GlcSph and XylSph.

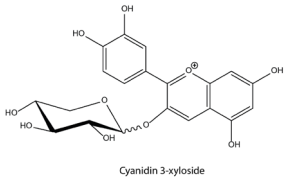

Supplemental Figure 3: Chemical structure Cyanidin 3-xyloside.

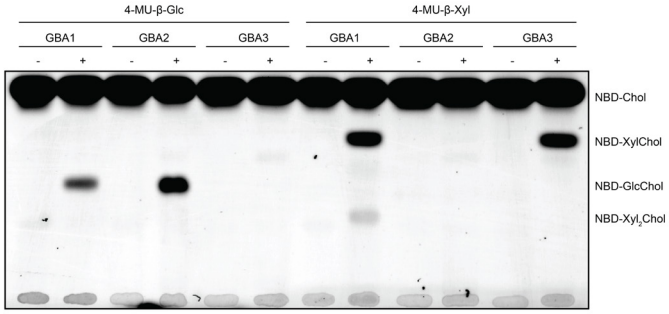

Supplemental Figure 4: Lack of transxylosylation by GBA2. HPTLC analysis of formation of glycosylated 25-NBD-cholesterol by β-glucosidases with 4-MU-β-Xyl and 4-MU-β-Glc as donor. Enzymes: recombinant hGCase; lysate of HEK293 cells overexpressing GBA2; lysate of HEK293 cells overexpressing GBA3. Incubation for 16 hours with (+) or without (-) enzyme preparation.

Supplemental Tables 1. MS/MS instrument parameters.

Mass spectrometer	Xevo-TQS-Micro (Waters)
Ionization mode	ESI+
Capillary voltage	3.50 kV
Source temperature	150 °C
Desolvation temperature	450 °C
Cone gas flow	50 L/h
Desolvation gas flow	950 L/h

Compound	Parent (m/z)	Daughter (m/z)	Cone voltage (V)	Collision energy (V)	RT (min)
GlcChol	566.5	369.3	20	15	1.34
^{13}C-GlcChol	572.0	369.3	20	15	1.34
XylChol	536.5	369.3	20	15	1.69
Xyl_2Chol	668.5	369.3	20	15	1.47
Xyl_3Chol	800.5	369.3	20	15	1.38
GlcSph	462.3	282.3	30	20	3.23
XylSph	432.67	282.3	25	15	3.25
C17-Sphinganine	288.3	270.3	20	15	3.26

References

1. E.A. Rennie, H.V. Scheller, Xylan biosynthesis, Curr Opin Biotechnol, 26 (2014) 100-107.
2. J.D. Esko, K. Kimata, U. Lindahl, Proteoglycans and Sulfated Glycosaminoglycans, in: nd, A. Varki, R.D. Cummings, J.D. Esko, H.H. Freeze, P. Stanley, C.R. Bertozzi, G.W. Hart, M.E. Etzler (Eds.) Essentials of Glycobiology, Cold Spring Harbor (NY), 2009.
3. J.L. Moriarity, K.J. Hurt, A.C. Resnick, P.B. Storm, W. Laroy, R.L. Schnaar, S.H. Snyder, UDP-glucuronate decarboxylase, a key enzyme in proteoglycan synthesis: cloning, characterization, and localization, J Biol Chem, 277 (2002) 16968-16975.
4. D. Fisher, P.W. Kent, Rat liver beta-xylosidase, a lysosomal membrane enzyme, Biochem J, 115 (1969) 50P-51P.
5. V. Patel, A.L. Tappel, Identity of beta-glucosidase and beta-xylosidase activities in rat liver lysosomes, Biochim Biophys Acta, 191 (1969) 86-94.
6. S. van Weely, M. Brandsma, A. Strijland, J.M. Tager, J.M. Aerts, Demonstration of the existence of a second, non-lysosomal glucocerebrosidase that is not deficient in Gaucher disease, Biochim Biophys Acta, 1181 (1993) 55-62.
7. E. Beutler, G.A. Grabowski, Gaucher disease, in: The Metabolic and Molecular Bases of Inherited Disease, McGraw-Hill Publishing Company, New York, United States, 1995, pp. 2641-2670.
8. M.J. Ferraz, W.W. Kallemeijn, M. Mirzaian, D. Herrera Moro, A. Marques, P. Wisse, R.G. Boot, L.I. Willems, H.S. Overkleeft, J.M. Aerts, Gaucher disease and Fabry disease: new markers and insights in pathophysiology for two distinct glycosphingolipidoses, Biochim Biophys Acta, 1841 (2014) 811-825.
9. H. Akiyama, S. Kobayashi, Y. Hirabayashi, K. Murakami-Murofushi, Cholesterol glucosylation is catalyzed by transglucosylation reaction of beta-glucosidase 1, Biochem Biophys Res Commun, 441 (2013) 838-843.
10. A.R. Marques, M. Mirzaian, H. Akiyama, P. Wisse, M.J. Ferraz, P. Gaspar, K. Ghauharali-van der Vlugt, R. Meijer, P. Giraldo, P. Alfonso, P. Irun, M. Dahl, S. Karlsson, E.V. Pavlova, T.M. Cox, S. Scheij, M. Verhoek, R. Ottenhoff, C.P. van Roomen, N.S. Pannu, M. van Eijk, N. Dekker, R.G. Boot, H.S. Overkleeft, E. Blommaart, Y. Hirabayashi, J.M. Aerts, Glucosylated cholesterol in mammalian cells and tissues: formation and degradation by multiple cellular beta-glucosidases, J Lipid Res, 57 (2016) 451-463.
11. H. Akiyama, Y. Hirabayashi, A novel function for glucocerebrosidase as a regulator of sterylglucoside metabolism, Biochim Biophys Acta Gen Subj, 1861 (2017) 2507-2514.
12. M.T. Vanier, Complex lipid trafficking in Niemann-Pick disease type C, J Inherit Metab Dis, 38 (2015) 187-199.
13. Y. Yildiz, H. Matern, B. Thompson, J.C. Allegood, R.L. Warren, D.M. Ramirez, R.E. Hammer, F.K. Hamra, S. Matern, D.W. Russell, Mutation of beta-glucosidase 2 causes glycolipid storage disease and impaired male fertility, J Clin Invest, 116 (2006) 2985-2994.
14. R.G. Boot, M. Verhoek, W. Donker-Koopman, A. Strijland, J. van Marle, H.S. Overkleeft, T. Wennekes, J.M. Aerts, Identification of the non-lysosomal glucosylceramidase as beta-glucosidase 2, J Biol Chem, 282 (2007) 1305-1312.
15. H.G. Korschen, Y. Yildiz, D.N. Raju, S. Schonauer, W. Bonigk, V. Jansen, E. Kremmer, U.B. Kaupp, D. Wachten, The non-lysosomal beta-glucosidase GBA2 is a non-integral membrane-associated protein at the endoplasmic reticulum (ER) and Golgi, J Biol Chem, 288 (2013) 3381-3393.
16. W.W. Kallemeijn, M.D. Witte, T.M. Voorn-Brouwer, M.T. Walvoort, K.Y. Li, J.D. Codee, G.A. van der Marel, R.G. Boot, H.S. Overkleeft, J.M. Aerts, A sensitive gel-based method combining distinct cyclophellitol-based probes for the identification of acid/base residues in human retaining beta-glucosidases, J Biol Chem, 289 (2014) 35351-35362.
17. M.D. Witte, W.W. Kallemeijn, J. Aten, K.Y. Li, A. Strijland, W.E. Donker-Koopman, A.M. van den Nieuwendijk, B. Bleijlevens, G. Kramer, B.I. Florea, B. Hooibrink, C.E. Hollak, R. Ottenhoff, R.G. Boot, G.A. van der Marel, H.S. Overkleeft, J.M. Aerts, Ultrasensitive in situ visualization of active glucocerebrosidase molecules, Nat Chem Biol, 6 (2010) 907-913.
18. S.P. Schroder, R. Petracca, H. Minnee, M. Artola, J.M.F.G. Aerts, J.D.C. Codee, G.A. van der Marel, H.S. Overkleeft, A Divergent Synthesis of L-arabino- and D-xylo-Configured Cyclophellitol Epoxides and Aziridines, Eur J Org Chem, (2016) 4787-4794.
19. W. Wiczkowski, E. Romaszko, M.K. Piskula, Bioavailability of cyanidin glycosides from natural chokeberry (Aronia melanocarpa) juice with dietary-relevant dose of anthocyanins in humans, J Agric Food Chem, 58 (2010) 12130-12136.
20. Y. Liu, D. Zhang, Y. Wu, D. Wang, Y. Wei, J. Wu, B. Ji, Stability and absorption of anthocyanins from blueberries subjected to a simulated digestion process, Int J Food Sci Nutr, 65 (2014) 440-448.
21. G.M. Aerts, O. Vanopstal, C.K. Debruyne, Beta-D-Glucosidase-Catalyzed Transfer of the Glycosyl Group

from Aryl Beta-D-Gluco-Pyranosides and Beta-D-Xylo-Pyranosides to Phenols, Carbohyd Res, 100 (1982) 221-233.
22. C.D. Kay, G. Mazza, B.J. Holub, J. Wang, Anthocyanin metabolites in human urine and serum, Br J Nutr, 91 (2004) 933-942.
23. C.L. Kuo, W.W. Kallemeijn, L.T. Lelieveld, M. Mirzaian, I. Zoutendijk, A. Vardi, A.H. Futerman, A.H. Meijer, H.P. Spaink, H.S. Overkleeft, J. Aerts, M. Artola, In vivo inactivation of glycosidases by conduritol B epoxide and cyclophellitol as revealed by activity-based protein profiling, FEBS J, 286 (2019) 584-600.
24. N. Dekker, T. Voorn-Brouwer, M. Verhoek, T. Wennekes, R.S. Narayan, D. Speijer, C.E. Hollak, H.S. Overkleeft, R.G. Boot, J.M. Aerts, The cytosolic beta-glucosidase GBA3 does not influence type 1 Gaucher disease manifestation, Blood Cells Mol Dis, 46 (2011) 19-26.
25. E. Uyama, K. Takahashi, M. Owada, R. Okamura, M. Naito, S. Tsuji, S. Kawasaki, S. Araki, Hydrocephalus, corneal opacities, deafness, valvular heart disease, deformed toes and leptomeningeal fibrous thickening in adult siblings: a new syndrome associated with beta-glucocerebrosidase deficiency and a mosaic population of storage cells, Acta Neurol Scand, 86 (1992) 407-420.
26. A. Chabas, B. Cormand, D. Grinberg, J.M. Burguera, S. Balcells, J.L. Merino, I. Mate, J.A. Sobrino, R. Gonzalez-Duarte, L. Vilageliu, Unusual expression of Gaucher's disease: cardiovascular calcifications in three sibs homozygous for the D409H mutation, J Med Genet, 32 (1995) 740-742.
27. A. Abrahamov, D. Elstein, V. Gross-Tsur, B. Farber, Y. Glaser, I. Hadas-Halpern, S. Ronen, M. Tafakjdi, M. Horowitz, A. Zimran, Gaucher's disease variant characterised by progressive calcification of heart valves and unique genotype, Lancet, 346 (1995) 1000-1003.
28. K.A. Karlsson, B.E. Samuelsson, G.O. Steen, Identification of a xylose-containing cerebroside in the salt gland of the herring gull, J Lipid Res, 13 (1972) 169-176.
29. W. Westbroek, M. Nguyen, M. Siebert, T. Lindstrom, R.A. Burnett, E. Aflaki, O. Jung, R. Tamargo, J.L. Rodriguez-Gil, W. Acosta, A. Hendrix, B. Behre, N. Tayebi, H. Fujiwara, R. Sidhu, B. Renvoise, E.I. Ginns, A. Dutra, E. Pak, C. Cramer, D.S. Ory, W.J. Pavan, E. Sidransky, A new glucocerebrosidase-deficient neuronal cell model provides a tool to probe pathophysiology and therapeutics for Gaucher disease, Dis Model Mech, 9 (2016) 769-778.
30. H.S. Overkleeft, G.H. Renkema, J. Neele, P. Vianello, I.O. Hung, A. Strijland, A.M. van der Burg, G.J. Koomen, U.K. Pandit, J.M. Aerts, Generation of specific deoxynojirimycin-type inhibitors of the non-lysosomal glucosylceramidase, J Biol Chem, 273 (1998) 26522-26527.
31. S. Ichikawa, H. Sakiyama, G. Suzuki, K.I. Hidari, Y. Hirabayashi, Expression cloning of a cDNA for human ceramide glucosyltransferase that catalyzes the first glycosylation step of glycosphingolipid synthesis, Proc Natl Acad Sci U S A, 93 (1996) 4638-4643.
32. J.M. Aerts, W.E. Donker-Koopman, M.K. van der Vliet, L.M. Jonsson, E.I. Ginns, G.J. Murray, J.A. Barranger, J.M. Tager, A.W. Schram, The occurrence of two immunologically distinguishable beta-glucocerebrosidases in human spleen, Eur J Biochem, 150 (1985) 565-574.
33. V.E. Ahn, P. Leyko, J.R. Alattia, L. Chen, G.G. Prive, Crystal structures of saposins A and C, Protein Sci, 15 (2006) 1849-1857.
34. J.M. Aerts, M.C. Sa Miranda, E.M. Brouwer-Kelder, S. Van Weely, J.A. Barranger, J.M. Tager, Conditions affecting the activity of glucocerebrosidase purified from spleens of control subjects and patients with type 1 Gaucher disease, Biochim Biophys Acta, 1041 (1990) 55-63.
35. E.G. Bligh, W.J. Dyer, A rapid method of total lipid extraction and purification, Can J Biochem Physiol, 37 (1959) 911-917.
36. J.E. Groener, B.J. Poorthuis, S. Kuiper, M.T. Helmond, C.E. Hollak, J.M. Aerts, HPLC for simultaneous quantification of total ceramide, glucosylceramide, and ceramide trihexoside concentrations in plasma, Clin Chem, 53 (2007) 742-747.
37. M. Mirzaian, P. Wisse, M.J. Ferraz, H. Gold, W.E. Donker-Koopman, M. Verhoek, H.S. Overkleeft, R.G. Boot, G. Kramer, N. Dekker, J.M. Aerts, Mass spectrometric quantification of glucosylsphingosine in plasma and urine of type 1 Gaucher patients using an isotope standard, Blood Cells Mol Dis, 54 (2015) 307-314.